

Extracting meson-baryon contributions to the electroexcitation of the $N(1675)_{\frac{5}{2}}^{-}$ nucleon resonance

I. G. Aznauryan^{1,2} and V. D. Burkert¹¹Thomas Jefferson National Accelerator Facility, Newport News, Virginia 23606, USA²A. I. Alikhanian National Science Laboratory (Yerevan Physics Institute), 0036 Yerevan, Armenia

(Received 8 December 2014; published 9 July 2015)

We report on the determination of the electrocouplings for the transition from the proton to the $N(1675)_{\frac{5}{2}}^{-}$ resonance state using recent differential cross section data on $ep \rightarrow e\pi^+n$ by the CLAS collaboration at $1.8 \leq Q^2 < 4.5 \text{ GeV}^2$. The data have been analyzed using two different approaches, the unitary isobar model and fixed- t dispersion relations. The extracted $\gamma^*p \rightarrow N(1675)_{\frac{5}{2}}^{-}$ helicity amplitudes show considerable coupling through the $A_{1/2}^p$ amplitude, that is significantly larger than the predicted three-quark contribution to this amplitude. The amplitude $A_{3/2}^p$ is much smaller. Both results are consistent with the predicted sizes of the meson-baryon contributions at $Q^2 \geq 1.8 \text{ GeV}^2$ from the dynamical coupled-channel model.

DOI: [10.1103/PhysRevC.92.015203](https://doi.org/10.1103/PhysRevC.92.015203)

PACS number(s): 13.60.Le, 13.40.Gp, 14.20.Gk, 25.30.Rw

I. INTRODUCTION

The excitation of nucleon resonances has been the subject of great interest since the development of the quark model in 1964 [1,2]. The proposed three-quark structure of the baryons when realized in the dynamical quark models resulted in prediction of a wealth of excited states with underlying spin-flavor and orbital symmetry of $SU(6) \otimes O(3)$. Most of the observed states have been found with hadronic probes, but they can also be investigated with electromagnetic probes [3]. From the excited states predicted by the quark model, only a fraction has been observed to date. The search for the “missing” states and more detailed studies of the resonance structure is now mostly carried out with electromagnetic probes and has been a major focus of hadron physics for the past decade [4]. This has led to a broad experimental effort in the development of large acceptance detectors and the measurement of exclusive meson photoproduction and electroproduction reactions, including many polarization observables. As a result, several new excited states of the nucleon have been discovered and entered into the Review of Particle Physics (RPP) [5]. Meson electroproduction revealed intriguing new information regarding the structure underlying the excited nucleon states [6].

One of the important insights is strong evidence that resonances are not excited from quark transitions alone, but there can be significant contributions from meson-baryon interactions as well, and that these two processes contribute to the excitation of the same state. This information has been obtained initially through the observation that the quark transition processes often do not have sufficient strength to explain fully the measured transition amplitudes and form factors. One of the best known examples is the photoexcitation of the $\Delta(1232)_{\frac{3}{2}}^{+}$ on the proton. This process is mostly due to a magnetic dipole transition from the nucleon, but only about 70% of the magnetic dipole transition form factor at the real photon point is explained by the quark content of the states. A more satisfactory description of the $\gamma^*p \rightarrow \Delta(1232)_{\frac{3}{2}}^{+}$ transition was achieved in models that incorporate pion-cloud contributions [7,8] and also in the dynamical reaction models, where the missing strength has been attributed to dynamical meson-baryon interaction in the final state [9–13].

The two main processes that contribute to the $\gamma^*N \rightarrow N^*$ transition are illustrated in Fig. 1 by the diagrams (a) and (b,c). The relative strength of these processes is determined by the dynamics of the quark interaction and $SU(6) \otimes O(3)$ structure of the N and N^* in the diagram of Fig. 1(a), as well by the meson-baryon coupling constants and dynamics of meson-baryon interaction in the diagrams of Figs. 1(b,c). The common feature of all approaches that account for meson-baryon contributions is the fact that these contributions are rapidly losing their strength when Q^2 increases. With electron scattering experiments, we have the tool to measure how the two contributions change their relative strength as a function of the distance scale, i.e., as we change Q^2 . Furthermore, at relatively small Q^2 , we have a unique handle to determine experimentally the non-quark contribution to $\gamma^*N \rightarrow N^*$, if excitation of the state through quark transition is suppressed. Most suitable for this purpose are measurements of the transition to resonant states with the total spin of the quarks $S_{3q} = \frac{3}{2}$ that belong to the $SU(6) \otimes O(3)$ multiplet [70,1⁻]. In the approximation of the single quark transition model (SQTM) [14–17], for the excitation of these states on proton, both transverse helicity amplitudes are suppressed, i.e., $A_{1/2}^p = A_{3/2}^p = 0$. This suppression is known as the “Moorhouse” selection rule [18], and is independent of Q^2 . The states with suppressed transverse amplitudes are $N(1650)_{\frac{1}{2}}^{-}$, $N(1675)_{\frac{5}{2}}^{-}$, and $N(1700)_{\frac{3}{2}}^{-}$. Two of them, $N(1650)_{\frac{1}{2}}^{-}$ and $N(1700)_{\frac{3}{2}}^{-}$, have partners in the same multiplet with the same quantum numbers, $N(1535)_{\frac{1}{2}}^{-}$ and $N(1520)_{\frac{3}{2}}^{-}$, for which the quark contributions are not suppressed. These states can mix. The mixing angle for the $N(1650)_{\frac{1}{2}}^{-}$ is large, approximately -31° [19,20], making it unsuitable as a candidate for a measurement of the nonquark components. The second state, $N(1700)_{\frac{3}{2}}^{-}$, has a much smaller mixing angle of about $+10^\circ$ and is a good candidate for such a measurement, if it can be separated experimentally from the $\Delta(1700)_{\frac{3}{2}}^{-}$. While this separation is possible with the data in at least two isospin configurations, e.g., $ep \rightarrow e\pi^+n$ and $ep \rightarrow e\pi^0p$, the π^0 data do not exist now in the energy range needed for investigation of the $N(1700)_{\frac{3}{2}}^{-}$ and $\Delta(1700)_{\frac{3}{2}}^{-}$ contributions. This leaves the $N(1675)_{\frac{5}{2}}^{-}$ as the sole suitable candidate for a measurement

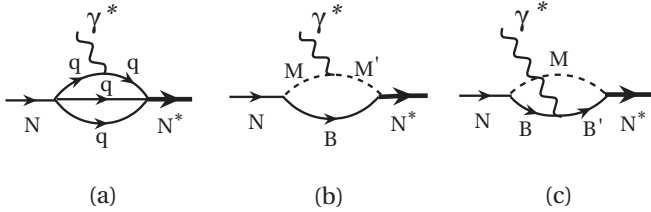


FIG. 1. Symbolic representation of the main contributions to the $\gamma^*N \rightarrow N^*$ transition: (a) through quark transition; (b,c) through meson-baryon pairs.

of the nonquark contributions to the transition amplitudes. The suppression of the transverse amplitudes for this state is also obtained in dynamical quark models that do not rely on the single quark approximation [21–23].

II. DATA ANALYSIS AND RESULTS

The results on the $\gamma^*p \rightarrow N(1675)_{\frac{5}{2}}^-$ transition reported in this paper have been extracted as part of global fits to over 37 000 cross section data points collected recently with CLAS on the $ep \rightarrow e\pi\pi^+$ at $1.8 \leq Q^2 < 4.5 \text{ GeV}^2$ and $1.60 < W < 2.0 \text{ GeV}$ [24]. To further constrain the analysis, these data were combined with the earlier CLAS data in the range $1.15 < W < 1.69 \text{ GeV}$ at close values of Q^2 [25]. Therefore, the data sets at each Q^2 covered four resonance regions from threshold to 2.0 GeV. Two conceptually different approaches, unitary isobar model (UIM) and dispersion relations (DR), were utilized in the analysis to model the nonresonant contributions which must be separated from the direct s -channel resonance contributions. These approaches were described in detail in Refs. [26,27] and have been successfully employed in Refs. [27–29] for analyses of pion electroproduction data in a wide range of Q^2 values from 0.16 to 6 GeV^2 .

The UIM [26,27] was developed on the basis of MAID [30]. At the values of Q^2 under investigation, the background of the UIM [26,27] is built from the nucleon exchanges in the s - and u -channels and t -channel π , ρ , and ω exchanges. This background is unitarized via unitarization of the multipole amplitudes in the K -matrix approximation. Resonance contributions are parametrized in the unified Breit-Wigner form with energy-dependent widths.

The DR approach [26,27] is based on fixed- t dispersion relations for invariant amplitudes. They relate real parts of the amplitudes to the Born term (s - and u -channel nucleon and t -channel π exchanges) and integral over imaginary parts of the amplitudes. Taking into account isotopic structure, there are 18 invariant amplitudes which describe π electroproduction on nucleons. For all these amplitudes, except one ($B_3^{(-)}$ in the notations of Refs. [26,27]), unsubtracted DR can be written. For $B_3^{(-)}$, the subtraction is necessary. At the values of Q^2 under investigation, the subtraction was found empirically in Ref. [27] from the description of the data [25]. This subtraction was successfully employed in the present analysis. In Ref. [26], the arguments were presented and discussed in detail, which show that in π electroproduction on nucleons, DR can be reliably used at $W \leq 1.8 \text{ GeV}$. The same conclusion was made

TABLE I. The values of χ^2 for the $\gamma^*p \rightarrow \pi^+n$ cross sections obtained in the analyses within UIM and DR. The data at $Q^2 = 1.8, 2.2, 2.6, 3.15, 4 \text{ GeV}^2$ and $Q^2 = 1.72, 2.05, 2.44, 2.91, 4.16 \text{ GeV}^2$ are, respectively, from Refs. [24,25].

Q^2 (GeV^2)	W (GeV)	Number of data points (N)	χ^2/N	
			UIM	DR
1.72	1.15–1.69	3530	2.7	2.9
1.8	1.6–2.01	8271	2.4	
	1.6–1.8	5602	2.3	2.4
2.05	1.15–1.69	5123	2.3	2.5
2.2	1.6–2.01	8140	2.2	
	1.6–1.8	5539	2.3	2.3
2.44	1.15–1.69	5452	2.0	2.3
2.6	1.6–2.01	7819	1.7	
	1.6–1.8	5373	2.0	2.2
2.91	1.15–1.69	5484	2.1	2.3
3.15	1.6–2.01	7507	1.8	
	1.6–1.8	5333	2.1	2.0
4.16	1.15–1.69	5778	1.2	1.3
4.0	1.6–2.01	5543	1.3	
	1.6–1.8	4410	1.5	1.6

in early applications of DR (see, for example, [31]). Therefore, in our DR analysis, the energy region is restricted by the first, second, and third resonance regions.

Both approaches, UIM and DR, give comparable descriptions of the data as is shown in Table I and Fig. 2.

In the global analysis, we have taken into account all four- and three-star resonances from the first, second, and third resonance regions: $\Delta(1232)_{\frac{3}{2}}^+$, $N(1440)_{\frac{1}{2}}^+$, $N(1520)_{\frac{3}{2}}^-$, $N(1535)_{\frac{1}{2}}^-$, $\Delta(1600)_{\frac{3}{2}}^+$, $\Delta(1620)_{\frac{1}{2}}^-$, $N(1650)_{\frac{1}{2}}^-$, $N(1675)_{\frac{5}{2}}^-$, $N(1680)_{\frac{5}{2}}^+$, $N(1700)_{\frac{3}{2}}^-$, $\Delta(1700)_{\frac{3}{2}}^-$, $N(1710)_{\frac{1}{2}}^+$, and $N(1720)_{\frac{3}{2}}^+$. From the resonances of fourth resonance region, we have included the resonances $\Delta(1905)_{\frac{5}{2}}^+$ and $\Delta(1950)_{\frac{7}{2}}^+$ which have been clearly seen in π photoproduction. For the masses, widths, and πN branching ratios of the resonances we used the mean values of the data from the RPP [5]. The results on the resonances of the first and second resonance regions including their model uncertainties are based on the data [25]. They have been found and presented in Ref. [27]. The analysis of the combined sets of data [24,25] allowed us to get reliable results for the electroexcitation amplitudes of the states $N(1675)_{\frac{5}{2}}^-$, $N(1680)_{\frac{5}{2}}^+$, and $N(1710)_{\frac{1}{2}}^+$. The isotopic pairs of the resonances $\Delta(1600)_{\frac{3}{2}}^+$ and $N(1720)_{\frac{3}{2}}^+$, $\Delta(1620)_{\frac{1}{2}}^-$ and $N(1650)_{\frac{1}{2}}^-$, $\Delta(1700)_{\frac{3}{2}}^-$ and $N(1700)_{\frac{3}{2}}^-$ could not be separated from each other from the data on the $N\pi$ production in one channel. For their investigation, data in at least two channels, e.g., $\gamma^*p \rightarrow n\pi^+$ and $\gamma^*p \rightarrow p\pi^0$, are necessary.

Here we present and discuss the results on the $N(1675)_{\frac{5}{2}}^-$, because of the unique role the state plays in the study of the meson-baryon contributions to the $\gamma^*N \rightarrow N^*$ transition amplitudes. Detailed results on the CLAS data and their global analysis have been presented in Ref. [24].

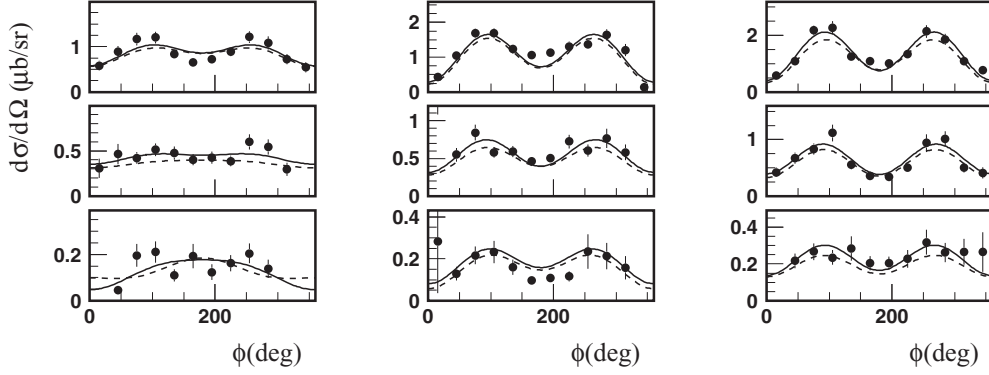


FIG. 2. Differential cross sections for the $\gamma^* p \rightarrow n\pi^+$ reaction at $W = 1.675$ GeV as a function of pion azimuthal angle ϕ at different values of pion polar angle θ . Data are from Ref. [24]. The rows correspond to $Q^2 = 1.8$ GeV², $\epsilon = 0.866$; $Q^2 = 2.6$ GeV², $\epsilon = 0.792$; $Q^2 = 4$ GeV², $\epsilon = 0.626$. The columns correspond to $\cos\theta = -0.5, 0.1, 0.5$. The solid (dashed) curves are the results obtained using UIM (DR) approach.

The results for the $\gamma^* p \rightarrow N(1675)_{\frac{5}{2}}^-$ transverse helicity amplitudes extracted from the experimental data are shown in Fig. 3. The presented amplitudes are averaged values of the results obtained using UIM and DR. The uncertainty that originates from the averaging is considered as one of the model uncertainties. We consider also two other kinds of model uncertainties. The first one arises from the uncertainties of the widths and masses of the resonances. The second one is related to the uncertainties of the background of UIM and the Born term in DR. The pion and nucleon electromagnetic form factors that enter these quantities are known quite well from experimental data [32–36], and the second uncertainty is caused mainly by the poor knowledge of the $\rho \rightarrow \pi\gamma$ form factor. According to the QCD sum rule [37] and quark model [38] predictions, the Q^2 dependence of this form factor is close to the dipole form $G_D(Q^2) = 1/(1 + \frac{Q^2}{0.71 \text{ GeV}^2})^2$. We used this form in our analysis and have introduced in

our final results a systematic uncertainty that accounts for a 20% deviation from 0.71 GeV². All these uncertainties added in quadrature are presented as model uncertainties of the amplitudes.

In Fig. 3, we show also the predictions of different quark models [21–23] that do not account for meson-baryon contributions. They are consistent with each other and confirm the strong suppression of the $\gamma^* p \rightarrow N(1675)_{\frac{5}{2}}^-$ transverse helicity amplitudes that follows from the SQTm [17]. The values of $A_{1/2}^p$ and $A_{3/2}^p$, predicted by quark models, are smaller than statistical and model uncertainties of the amplitudes extracted from the data [24,25]. Therefore, taking into account these uncertainties, the experimental $\gamma^* p \rightarrow N(1675)_{\frac{5}{2}}^-$ amplitudes can be considered as determined predominantly by the contributions caused by meson-baryon effects. The extracted amplitudes show significant coupling through $A_{1/2}^p$, while $A_{3/2}^p$ is consistent with 0 within statistical and model uncertainties.

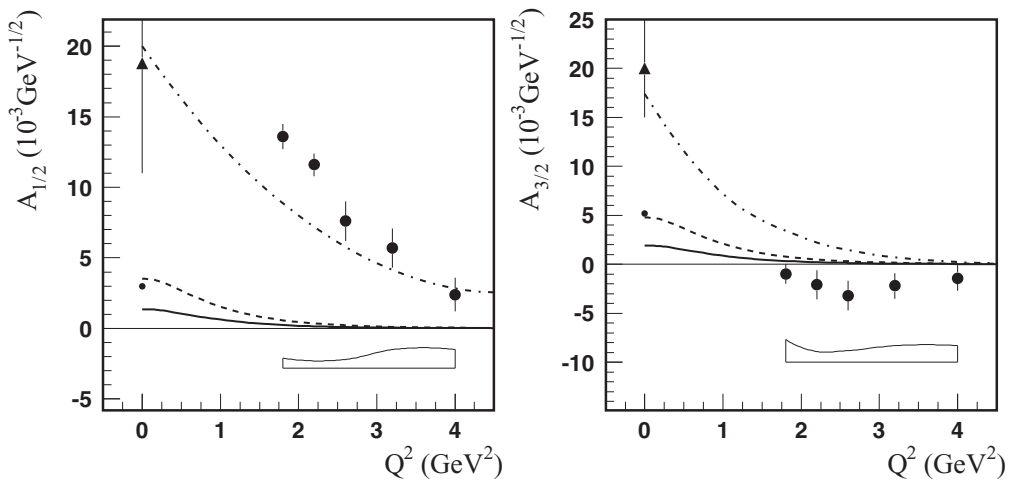


FIG. 3. Transverse helicity amplitudes for the $\gamma^* p \rightarrow N(1675)_{\frac{5}{2}}^-$ transition. The full circles are the amplitudes extracted from the data [24,25] using the following mass, width, and πN branching ratio of the resonance: $M = 1.675$ GeV, $\Gamma = 0.15$ GeV, and $\beta_{\pi N} = 0.4$. The bands show the model uncertainties. The full triangles at $Q^2 = 0$ are the RPP estimates [5]. The solid and dashed curves correspond to quark model predictions of Refs. [22] and [23], respectively; the dots at $Q^2 = 0$ are the predictions of the light-front relativistic quark model from Ref. [21]. Dashed-dotted curves are absolute values of the predicted meson-baryon contributions from the dynamical coupled-channel model of Ref. [13].

Taking into account values of the amplitudes at $Q^2 = 0$ [5], we conclude that $A_{3/2}^p$ drops much faster than $A_{1/2}^p$.

In Fig. 3, we show the results from the dynamical coupled-channel approach by the EBAC group [13]. In this approach the meson-baryon contributions to the $\gamma^*p \rightarrow N(1675)_{\frac{5}{2}}^{-}$ amplitudes have been found at the resonance pole position. The amplitudes that are presented in Fig. 3 are absolute values of these contributions continued to the real axis close to the mass of the state $N(1675)_{\frac{5}{2}}^{-}$. Q^2 behavior of the amplitudes extracted from experiment and their sizes are qualitatively consistent with these results of the dynamical coupled-channel approach [13].

III. SUMMARY

Based on new high precision data from CLAS in the $ep \rightarrow e\pi^+n$ channel [24], combined with previously obtained data on the same channel at close values of Q^2 but at lower values of W [25], we have extracted the electroexcitation helicity amplitudes for the resonance $N(1675)_{\frac{5}{2}}^{-}$. A special feature of this state is the strong suppression of the transverse helicity amplitudes for its excitation through quark transition from the

proton. This feature allowed us to draw conclusions regarding the dominant strength of the meson-baryon contributions to the $\gamma^*p \rightarrow N(1675)_{\frac{5}{2}}^{-}$ transition. The results are important as unambiguous experimental test for models that account for the meson-baryon contributions to the electroexcitation of nucleon resonances and will support theoretical developments towards a more complete understanding of the dynamics of nucleon resonance excitations.

The data [24,25] cover the relatively high Q^2 range. It would be desirable to study the state $N(1675)_{\frac{5}{2}}^{-}$ at lower Q^2 to map out the transition to the real photon point where the amplitudes are not well known. Furthermore, measurements on the neutron are very desirable, as significant strength through quark transition is expected for both transverse amplitudes in the excitation of the $N(1675)_{\frac{5}{2}}^{-}$ from the neutron [17].

ACKNOWLEDGMENTS

This work was supported by the State Committee of Science of Republic of Armenia, Grant No. 13-1C023, and the U.S. Department of Energy, Office of Science, Office of Nuclear Physics, under Contract No. DE-AC05-06OR23177.

-
- [1] M. Gell-Mann, *Phys. Lett.* **8**, 214 (1964).
 [2] G. Zweig, CERN Report Nos. TH 401 and 412 (1964).
 [3] L. A. Copley, G. Karl, and E. Obryk, *Nucl. Phys. B* **13**, 303 (1969).
 [4] V. D. Burkert and T.-S. H. Lee, *Int. J. Mod. Phys. E* **13**, 1035 (2004).
 [5] K. A. Olive *et al.* (Particle Data Group), *Chin. Phys. C* **38**, 090001 (2014).
 [6] I. G. Aznauryan and V. D. Burkert, *Prog. Part. Nucl. Phys.* **67**, 1 (2012).
 [7] D. H. Lu, A. W. Thomas, and A. G. Williams, *Phys. Rev. C* **55**, 3108 (1997).
 [8] A. Faessler, T. Gutsche, B. R. Holstein, V. E. Lyubovitskij, D. Nicmorus, and K. Pumsard, *Phys. Rev. D* **74**, 074010 (2006).
 [9] S. S. Kamalov and S. N. Yang, *Phys. Rev. Lett.* **83**, 4494 (1999).
 [10] S. S. Kamalov, S. Nan Yang, D. Drechsel, O. Hanstein, and L. Tiator, *Phys. Rev. C* **64**, 032201(R) (2001).
 [11] T. Sato and T.-S. H. Lee, *Phys. Rev. C* **63**, 055201 (2001).
 [12] A. Matsuyama, T. Sato, and T.-S. H. Lee, *Phys. Rep.* **439**, 193 (2007).
 [13] B. Juliá-Díaz, T.-S. H. Lee, A. Matsuyama, T. Sato, and L. C. Smith, *Phys. Rev. C* **77**, 045205 (2008).
 [14] A. J. G. Hey and J. Weyers, *Phys. Lett. B* **48**, 69 (1974).
 [15] J. Babcock and J. L. Rosner, *Ann. Phys. (NY)* **96**, 191 (1976).
 [16] W. N. Cottingham and I. H. Dunbar, *Z. Phys. C* **2**, 41 (1979).
 [17] V. D. Burkert, R. De Vita, M. Battaglieri, M. Ripani, and V. Mokeev, *Phys. Rev. C* **67**, 035204 (2003).
 [18] R. G. Moorhouse, *Phys. Rev. Lett.* **16**, 772 (1966).
 [19] N. Isgur and G. Karl, *Phys. Lett. B* **72**, 109 (1977).
 [20] A. J. G. Hey, P. J. Litchfield, and R. J. Cashmore, *Nucl. Phys. B* **95**, 516 (1975).
 [21] I. G. Aznauryan and A. S. Bagdasaryan, *Yad. Fiz.* **41**, 249 (1985) [*Sov. J. Nucl. Phys.* **41**, 158 (1985)].
 [22] E. Santopinto and M. M. Giannini, *Phys. Rev. C* **86**, 065202 (2012).
 [23] D. Merten, U. Löring, B. Metsch, and H. Petry, *Eur. Phys. J. A* **18**, 193 (2003).
 [24] K. Park *et al.* (CLAS Collaboration), *Phys. Rev. C* **91**, 045203 (2015).
 [25] K. Park *et al.* (CLAS Collaboration), *Phys. Rev. C* **77**, 015208 (2008).
 [26] I. G. Aznauryan, *Phys. Rev. C* **67**, 015209 (2003).
 [27] I. G. Aznauryan *et al.* (CLAS Collaboration), *Phys. Rev. C* **80**, 055203 (2009).
 [28] I. G. Aznauryan, V. D. Burkert, H. Egiyan, K. Joo, R. Minehart, and L. C. Smith, *Phys. Rev. C* **71**, 015201 (2005).
 [29] I. G. Aznauryan, V. D. Burkert, G. V. Fedotov, B. S. Ishkhanov, and V. I. Mokeev, *Phys. Rev. C* **72**, 045201 (2005).
 [30] D. Drechsel, O. Hanstein, S. Kamalov, and L. Tiator, *Nucl. Phys. A* **645**, 145 (1999).
 [31] R. L. Crawford, *Nucl. Phys. B* **97**, 125 (1975).
 [32] J. Arrington, W. Melnitchouk, and J. A. Tjon, *Phys. Rev. C* **76**, 035205 (2007).
 [33] J. Lachniet *et al.* (CLAS Collaboration), *Phys. Rev. Lett.* **102**, 192001 (2009).
 [34] T. Horn *et al.*, *Phys. Rev. Lett.* **97**, 192001 (2006).
 [35] V. Tadevosyan *et al.*, *Phys. Rev. C* **75**, 055205 (2007).
 [36] S. Riordan *et al.*, *Phys. Rev. Lett.* **105**, 262302 (2010).
 [37] V. Eletski and Ya. Kogan, *Yad. Fiz.* **39**, 138 (1984).
 [38] I. Aznauryan and K. Oganessyan, *Phys. Lett. B* **249**, 309 (1990).